Role of the loop $L_{4,5}$ in allosteric regulation in mtHsp70s: in vivo significance of domain communication and its implications in protein translocation

Madhuja Samaddar, Arvind Vittal Goswami*, Jaya Purushotham, Pushpa Hegde†, and Patrick D'Silva
Department of Biochemistry, Indian Institute of Science, Bangalore 560012, India

ABSTRACT **Mitochondrial Hsp70 (mtHsp70) is essential for a vast repertoire of functions, including protein import, and requires effective interdomain communication for efficient partner-protein interactions. However, the in vivo functional significance of allosteric regulation in eukaryotes is poorly defined. Using integrated biochemical and yeast genetic approaches, we provide compelling evidence that a conserved substrate-binding domain (SBD) loop, $L_{4,5}$, plays a critical role in allosteric communication governing mtHsp70 chaperone functions across species. In yeast, a temperature-sensitive $L_{4,5}$ mutation (E467A) disrupts bidirectional domain communication, leading to compromised protein import and mitochondrial function. Loop $L_{4,5}$ functions synergistically with the linker in modulating the allosteric interface and conformational transitions between SBD and the nucleotide-binding domain (NBD), thus regulating interdomain communication. Second-site intragenic suppressors of E467A isolated within the SBD suppress domain communication defects by conformationally altering the allosteric interface, thereby restoring import and growth phenotypes. Strikingly, the suppressor mutations highlight that restoration of communication from NBD to SBD alone is the minimum essential requirement for effective in vivo function when primed at higher basal ATPase activity, mimicking the J-protein–bound state. Together these findings provide the first mechanistic insights into critical regions within the SBD of mtHsp70s regulating interdomain communication, thus highlighting its importance in protein translocation and mitochondrial biogenesis.**

Monitoring Editor
Thomas D. Fox
Cornell University

Received: Mar 21, 2014
Revised: May 8, 2014
Accepted: May 8, 2014

INTRODUCTION

Mitochondria are essential eukaryotic organelles and important centers for several biochemical reactions, including metabolic energy generation by oxidative phosphorylation. They are double membrane–bound complex organelles containing their own genome, which encodes for 8 and 13 proteins in yeast and humans, respectively (Sickmann *et al.*, 2003; Taylor and Turnbull, 2005). Greater than 98% of mitochondrial proteins are encoded by the nuclear genome and synthesized on cytosolic ribosomes. The biogenesis of functional mitochondria thus requires efficient import of several hundred proteins through well-defined transport machinery of the outer and inner membranes, which are highly conserved across phylogenetic boundaries (Neupert *et al.*, 1990; Pfanner and Geissler, 2001).

The polypeptides destined for the mitochondrial compartment are guided through their signal sequences, which are initially recognized by the translocase of the outer membrane (TOM) complex. The amino-terminal matrix-targeting signal (MTS) sequence–containing proteins are further recognized by the translocase of the inner membrane (TIM) complex (Rehling *et al.*, 2001;

This article was published online ahead of print in MBoC in Press (http://www.molbiolcell.org/cgi/doi/10.1091/mbc.E14-03-0821) on May 14, 2014.

Present addresses: *Department of Pathology, Yale School of Medicine, New Haven, CT 06520; †Institut National de la Santé et de la Recherche Médicale, Unité 872, Centre de Recherche des Cordeliers, 75006 Paris, France.

Address correspondence to: Patrick D'Silva (patrick@biochem.iisc.ernet.in).

Abbreviations used: DHFR, dihydrofolate reductase; F-P5, fluorescein-labeled P5 peptide; IP, immunoprecipitation; mtHsp70, mitochondrial Hsp70; NBD, nucleotide-binding domain; SBD, substrate-binding domain.

Neupert and Brunner, 2002). More than 60% of proteins containing the presequence are translocated through an essential inner membrane–bound presequence translocase whose components are highly conserved among eukaryotes. It is organized as a central membrane-bound translocation channel comprising Tim23, Tim17, Tim50, and Tim21 subunits (Neupert and Herrmann, 2007). The translocase consists of a terminal dynamic import motor subcomplex composed of mitochondrial Hsp70 (mtHsp70; Ssc1 in yeast) at its core, recruited by the peripheral membrane protein Tim44, which tethers it to the translocation channel for binding incoming polypeptides (Neupert and Brunner, 2002). The import process is facilitated by a J-protein subcomplex, the Pam18–Pam16 heterodimer, which stimulates ATP hydrolysis of mtHsp70 coupled with translocation of polypeptides into the matrix compartment (Truscott *et al.*, 2003; D'Silva *et al.*, 2005, 2008). The membrane potential gradient ($\Delta\Psi$) across the inner membrane is required for initial insertion of the MTS of a preprotein into the Tim23 channel (Geissler *et al.*, 2000). The actual inward movement of the polypeptide is driven by the motor function of mtHsp70, powered through ATP hydrolysis in multiple rounds of a chaperone cycle (Voos *et al.*, 1996; Voisine *et al.*, 1999).

In eukaryotic systems, the mtHsp70s (orthologues of DnaK) play a pivotal role in the import and folding of proteins destined for various mitochondrial subcompartments. Hence it is a critical determinant of mitochondrial biogenesis, integrity, and function. In *Saccharomyces cerevisiae,* mitochondria contain three Hsp70 paralogues, namely Ssc1, Ssq1, and Ssc3 (Craig and Marszalek, 2002). Of these, Ssc1 (mtHsp70) is the major chaperone essential for protein import, as well as for its quality control, thus playing a critical role in biogenesis of the organelle (Kang *et al.*, 1990). The cochaperones Mdj1 and Mge1 (orthologues of bacterial DnaJ and GrpE) assist Ssc1 in its folding and protein import functions (Laloraya *et al.*, 1994; Rowley *et al.*, 1994; Jordan and McMacken, 1995). The Ssq1 paralogue is involved in specialized functions, such as iron–sulfur cluster biogenesis (Craig and Marszalek, 2002). Although the Ssc3 paralogue possesses a high degree of sequence similarity with Ssc1, it does not complement the essential functions of Ssc1 (Pareek *et al.*, 2011). In contrast, in humans, mitochondria contain a single mtHsp70 (Grp75/mortalin), performing a vast array of crucial physiological functions (Kaul *et al.*, 2007) with the aid of cochaperones such as J-protein, Tid1, and the nucleotide exchange factor GrpEL1 (Goswami *et al.*, 2010).

Like other general Hsp70s, the chaperone cycle of mitochondrial Hsp70 is modulated by two core activities. The C-terminal substrate-binding domain (SBD) interacts with polypeptide substrates, and its binding affinity is regulated by a 10-kDa α-helical lid region (Strub *et al.*, 2003). On the other hand, the N-terminal nucleotide-binding domain (NBD) binds to nucleotides and undergoes a cycle of ATP hydrolysis in response to substrate capture (McCarty *et al.*, 1995). Therefore the chaperone cycle is characterized by multiple cycles of substrate binding and release coupled to ATP binding and hydrolysis, based on effective interdomain communication mediated by conformational transitions between them. In addition, the mtHsp70 chaperone cycle is assisted by cochaperones, which enable the transitions between the two nucleotide-bound states. The J-proteins (Hsp40s) stimulate the ATP-hydrolyzing activity of mtHsp70s, thus stabilizing interactions with substrates in the ADP-bound state. The nucleotide exchange factors are involved in the exchange of bound ADP by ATP, thereby repriming mtHsp70s for multiple further rounds of folding cycles (Liberek *et al.*, 1991a).

An interdomain allosteric communication is critical for effective Hsp70 chaperone function. In Hsp70s, the NBD and SBD are connected via a highly conserved linker region, which is important for maintaining the interdomain interface (Swain *et al.*, 2007). The ATPase and substrate-binding activities are mutually coordinated by bidirectional interdomain communication between the domains. Binding of ATP and its hydrolysis at the NBD brings conformational changes, thereby modulating the substrate affinity at the SBD (Szabo *et al.*, 1994). Conversely, substrate binding to the SBD stimulates ATP hydrolysis at the NBD (Mayer and Bukau, 2005). The critical process of allosteric regulation in Hsp70 proteins has been investigated in the bacterial Hsp70 homologue, DnaK. Recent structural analyses provide mechanistic insights into its interactions with ligands and cochaperones, and structure and conformational transitions in various ligand-bound states (Swain *et al.*, 2007; Bertelsen *et al.*, 2009; Bhattacharya *et al.*, 2009; Liebscher and Roujeinikova, 2009; Kityk *et al.*, 2012; Zhuravleva *et al.*, 2012; Qi *et al.*, 2013). In addition, some of the important contact regions between the two domains that are required for allosteric regulation have been uncovered (Montgomery *et al.*, 1999; Vogel *et al.*, 2006a,b; Zhuravleva *et al.*, 2012). However, the mechanism of bidirectional interdomain communication and conformational transitions in different nucleotide bound states is not well defined.

Although mtHsp70s have a high degree of sequence similarities with bacterial DnaK, they are highly evolved and possess significant differences in their conformational and biochemical properties (Jiang *et al.*, 2005; Moro *et al.*, 2005; Mapa *et al.*, 2010). Moreover, they are essential for a vast repertoire of physiological functions, which are distinctly different from those of their bacterial counterpart. Owing to the lack of suitable conditional mutants, the significance of interdomain communication in mtHsp70s for specific protein translocation functions, such as recruitment to the membrane tether, Tim44, is elusive. In addition, the extent of in vivo tolerance of an interdomain defect without compromising physiological functions is unclear in eukaryotic systems. In this article, using yeast genetic approaches, we systematically elucidate the regions of the SBD that are critical for allosteric regulation and its relevance for protein import, as well as for mitochondrial biogenesis. Our findings show that a conserved SBD loop, $L_{4,5}$ in mtHsp70s, plays a significant role in allosteric communication in yeast, as well as in the mammalian system. The loop $L_{4,5}$ functions synergistically with the linker region in organizing the interdomain interface and propagating bidirectional communication. The intragenic suppressors isolated within the SBD provide invaluable in vivo evidence toward understanding the mechanisms governing interdomain communication relevant to protein import and mitochondrial functions in eukaryotic model systems.

RESULTS

Conserved SBD loop $L_{4,5}$ modulates interdomain communication in mtHsp70 proteins across species

Mutations in human mtHsp70 have been associated with varied disease conditions, including cancer, neurodegeneration, and myelodysplastic syndrome (MDS). Previous reports showed that a point mutation in the SBD, $mtHsp70_{G489E}$, is associated with myelodysplastic syndrome (Craven *et al.*, 2005), with a unique set of altered biochemical properties. These include fivefold elevated basal rate of ATP hydrolysis and 70% loss in stimulation of ATPase activity by peptide substrates (Goswami *et al.*, 2010), both of which are hallmarks of interdomain communication defects. This residue, G489, is located in a loop $L_{4,5}$ that is involved in stabilizing the substrate-binding pocket (Figure 1A), and a comparative sequence analysis revealed that the amino acids in loop $L_{4,5}$ were highly conserved in multiple Hsp70 proteins across species (Figure 1B and Supplemental Figure S1). This observation led us to investigate the

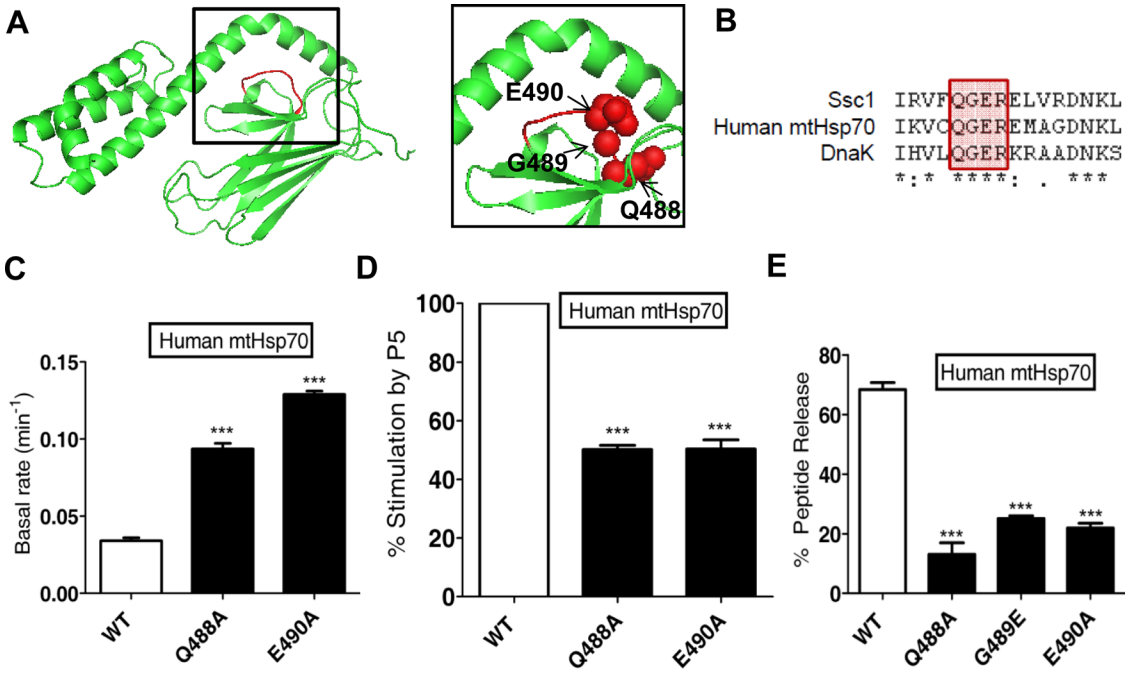

FIGURE 1: Effects of mutations in loop $L_{4,5}$ of human mtHsp70. (A) Modeled structure of human mtHsp70 SBD depicting the position of loop $L_{4,5}$ (highlighted in red). The side chains of individual amino acid residues mutated from this loop are shown in the inset. (B) Multiple sequence alignment showing the conservation of loop $L_{4,5}$ in multiple Hsp70 proteins. The loop residues QGER are highlighted in the alignment. (C) Measurement of basal ATPase activity. The preformed labeled human mtHsp70[ATP] complexes of wild type and loop $L_{4,5}$ mutants were subjected to single-turnover ATPase assays as described in *Materials and Methods*. The percentage conversion of ATP to P_i as a function of time was used to determine the rate of hydrolysis. (D) Stimulation of ATPase activity by P5 peptide. The complexes were subjected to the ATPase assay in the presence of 250-fold molar excess of P5 peptide to determine extent of stimulation and represented as a bar chart after normalization of the values. (E) Estimation of ATP-induced substrate release by fluorescence anisotropy. ATP, 5 mM, was added to 20 μM preformed mtHsp70[F-P5] complexes of wild type or the loop $L_{4,5}$ mutants. Release of bound F-P5 was monitored as a function of decrease in anisotropy value up to 5 min post–ATP addition.

role of this loop in regulating interdomain communication in mtHsp70 proteins across species.

To examine whether other residues from the conserved loop $L_{4,5}$ also play a role in allosteric communication between domains, we generated site-directed mutations at two residues adjacent to G489 and purified them from *Escherichia coli* BL21 by coexpression with yeast Zim17 (Blamowska *et al.*, 2010; Goswami *et al.*, 2010). The mutant mtHsp70$_{Q488A}$ showed a 2.75-fold increment, and mtHsp70$_{E490A}$ led to a 3.8-fold enhancement in the basal ATPase activity (Figure 1C). Both mutants also displayed a marked decrease in stimulation of ATPase activity by P5 substrate peptide, similar to mtHsp70$_{G489E}$ (Figure 1D). Furthermore, all three loop $L_{4,5}$ mutant proteins showed >50% reduction in the release of prebound substrate upon ATP binding as compared with wild type (Figure 1E). Although lowered stimulation of ATPase activity by substrates indicates disruption of communication from SBD to NBD, decrease in substrate release by ATP reflects lack of signal transfer from NBD to SBD. Thus mutants from the loop $L_{4,5}$ in human mtHsp70 demonstrate impairment in bidirectional allosteric communication.

Further, to investigate the in vivo functional significance of a loop $L_{4,5}$ in domain communication and protein import, we generated the analogous mutations in *S. cerevisiae* mtHsp70 (Ssc1), which displays 82% sequence similarity with its human counterpart. The transformed yeast strains were subjected to 5-fluoroorotic acid (5-FOA) counterselection in order to eliminate the wild-type *SSC1* plasmid required for strain viability and tested for the effect of the mutations. The Ssc1 counterpart of the MDS mutant, G466E, was found to be lethal and unable to grow on 5-FOA medium (Figure 2A). The mutants Q465A and E467A were both viable at 30°C but displayed temperature sensitivity at 34 and 37°C (Figure 2B). To test their biochemical properties, we coexpressed the mutants with yeast Zim17 and purified them using the *E. coli* system (Goswami *et al.*, 2012). Remarkably, all three mutants (G466E, Q465A, and E467A) in yeast Ssc1 showed conserved alterations in biochemical properties similar to their human counterparts. Whereas G466E exhibited a drastic 11-fold increase in basal ATPase activity, the Q465A and E467A proteins showed 2.25- and 4.85-fold enhancements, respectively (Figure 2C). In addition, communication-specific assays revealed that all three mutants exhibited ~70% reduction in stimulation of ATPase activity by substrate as compared with wild type (Figure 2D). The mutants also showed ~50% reduction in release of prebound substrate upon ATP binding (Figure 2E). To further validate the communication defects in mutants, we used an intrinsic fluorescence quenching method similar to *E. coli* DnaK. It is known that ATP binding induces rearrangements of the NBD subdomains, leading to conformational changes in the SBD, which open the substrate-binding pocket by displacing the helical lid. The subdomain movements can be directly monitored by ATP-induced changes in the fluorescence of the single tryptophan residue in the NBD (Buchberger *et al.*, 1995; Montgomery *et al.*, 1999). Consistent with other assays, Q465A and E467A mutants exhibited >25% reduction in tryptophan fluorescence quenching upon ATP binding,

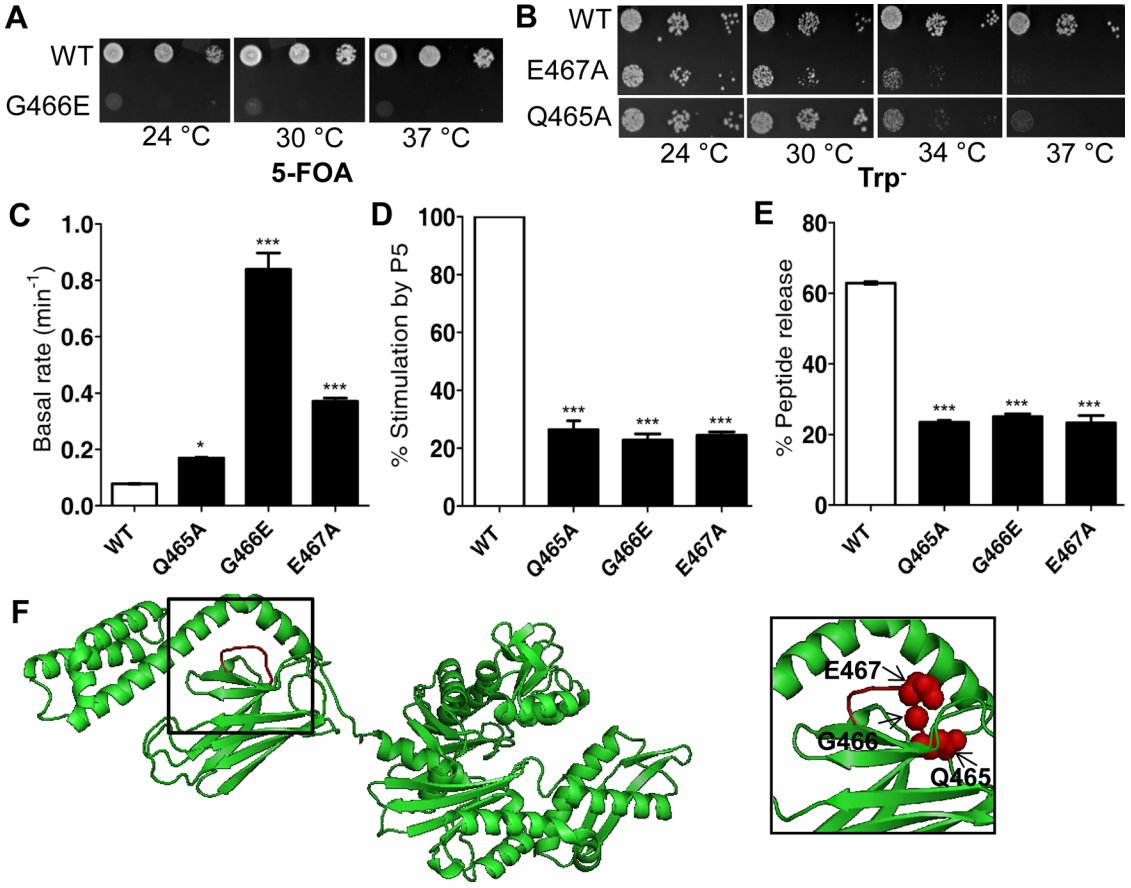

FIGURE 2: Growth phenotypes and biochemical defects associated with analogous mutations in the loop $L_{4,5}$ of yeast Ssc1. (A) Effect of G466E mutation on growth. Yeast cells transformed with pRS314-*ssc1*$_{G466E}$ were subjected to 10-fold serial dilutions and spotted on minimal medium containing 5-FOA. The plates were incubated at the indicated temperatures for 96 h. (B) Growth phenotype analysis of E467A and Q465A mutants. Cells equivalent to 1 OD at A_{600} from each yeast strain were subjected to 10-fold serial dilutions, followed by spotting on minimal medium and incubation for 65 h at indicated temperature conditions. (C) Estimation of basal ATPase activity. The preformed labeled Ssc1[ATP] complexes of wild type and loop $L_{4,5}$ mutants were subjected to single-turnover assays to determine their intrinsic ATPase activities as described in *Materials and Methods*. (D) Determination of ATPase activity upon stimulation by P5 peptide. The labeled Ssc1[ATP] complexes were subjected to ATPase activity measurements in the presence of 100-fold molar excess of P5 peptide to measure the efficiency of stimulation. The normalized values are represented in a bar chart. (E) Comparison of ATP-induced substrate release by fluorescence anisotropy. ATP, 2.5 mM, was added to 5 µM wild-type or mutant Ssc1[F-P5] complexes, and the decrease in anisotropy was monitored. The total percentage decrease in anisotropy value 5 min post–ATP addition is represented. (F) Modeled structure of full-length Ssc1 depicting the position of loop $L_{4,5}$ (highlighted in red). The side chains of individual amino acid residues mutated are shown in the inset.

thus confirming the allosteric defects (Supplemental Figure S2). The position of the loop $L_{4,5}$ in the modeled structure of mtHsp70 (Figure 2F) indicates its proximity to both the helical lid region and the interface of the NBD and SBD, thus regulating the synchronized functions of both domains. In summary, the findings of the analyses from both yeast and human mtHsp70 mutants suggest that the loop $L_{4,5}$ plays a critical role in mtHsp70s to maintain the allosteric bidirectional communication governing its biochemical activities.

Intragenic suppressors within the SBD can rescue growth phenotype and substrate interactions

To demonstrate in vivo the critical nature of loop $L_{4,5}$ in regulating interdomain communication, we performed a mutagenic screen for isolating intragenic suppressors against the E467A mutant. This mutant was selected based on its higher basal ATPase activity in comparison to Q465A and distinct lack of growth at 37°C. To obtain intragenic suppressors, we generated a mutagenic library by error-prone PCR. The nucleotide sequence spanning the *SSC1* substrate-binding domain and containing the E467A mutation was used as a template for this purpose. The mutagenic library was transformed into Δ*ssc1* haploid strain harboring a functional copy of *SSC1* gene on a *URA3*-based plasmid. Screening of suitable suppressors capable of rescuing the mutant phenotype was performed by selecting the transformants on 5-FOA medium and testing for growth at the nonpermissive temperature of 37°C. Based on our genetic screen, eight unique changes at four different amino acid locations were identified within the SBD that could suppress the growth defect of E467A. These are K490R (S209), N508K/T (S205, S207), D519G/E/N/Y (S208, S201, S204, S203), and V524I (S202; Figure 3A and Supplemental Table S1). All are located in the β-sheet region of the substrate-binding pocket, except K490, which is located in loop $L_{5,6}$ (Figure 3C). All the intragenic suppressors could rescue the

A

Suppressor Name	Genetic composition
S201	E467A - D519E
S202	E467A - V524I
S203	E467A - D519Y
S204	E467A - D519N
S205	E467A - N508K
S207	E467A - N508T
S208	E467A - D519G
S209	E467A - K490R

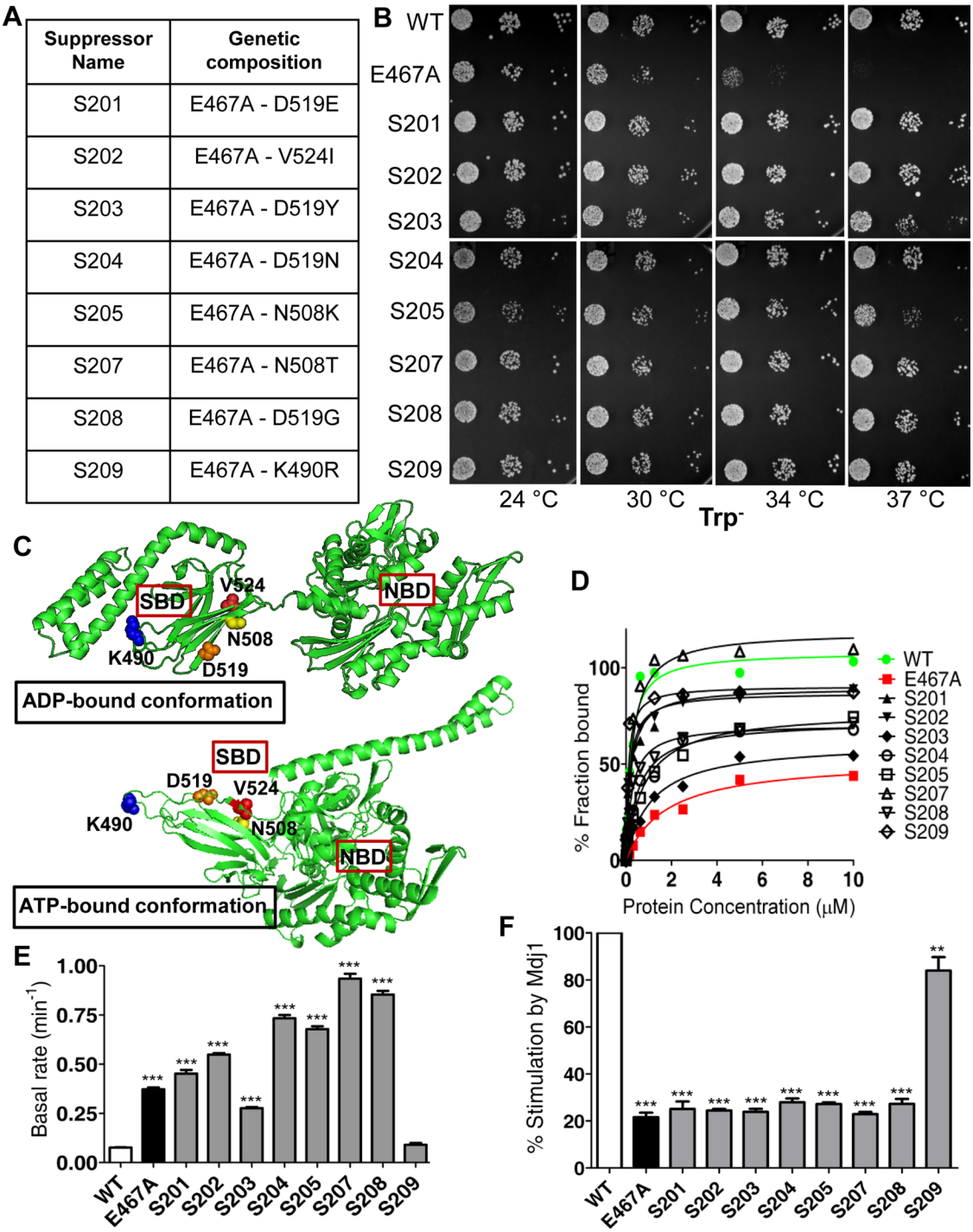

FIGURE 3: Identification and biochemical characterization of intragenic suppressors of E467A. (A) Summary of the suppressor mutations of E467A identified by mutagenic screening. The suppressors are referred to as S201–S209, and corresponding amino acid substitutions are indicated. (B) Growth phenotype analysis. Cells equivalent to 1 OD at A_{600} from each yeast strain were serially diluted, spotted on minimal medium, and incubated at indicated temperatures for 65 h. (C) Mapping the location of suppressor mutations. The positions of the suppressor mutations are indicated in the modeled structure of Ssc1 in the ADP-bound (top) and ATP-bound (bottom) conformations. The side chains of the corresponding amino acid residues are denoted as colored spheres. (D) Estimation of substrate-binding affinities of the suppressor proteins. Increasing concentrations of the wild-type, mutant, and suppressor proteins were incubated with 25 nM F-P5 peptide for 1 h at 25°C. After binding reached equilibrium, the anisotropy values were recorded and fitted to a one-site binding equation in GraphPad Prism 5.0 to obtain the K_d values. (E) Measurement of basal ATPase activities of suppressor proteins. The basal rates of hydrolysis of E467A and its suppressors were estimated by single-turnover ATPase assays with preformed labeled Ssc1[ATP] complexes as described in *Materials and Methods*. (F) Stimulation of basal ATPase activity by Mdj1. Labeled Ssc1[ATP] complexes of wild type, E467A, and suppressors were subjected to single-turnover assays in the presence of twofold molar excess Mdj1 protein. Efficiency of stimulation was normalized and represented, setting the wild-type value as 100%.

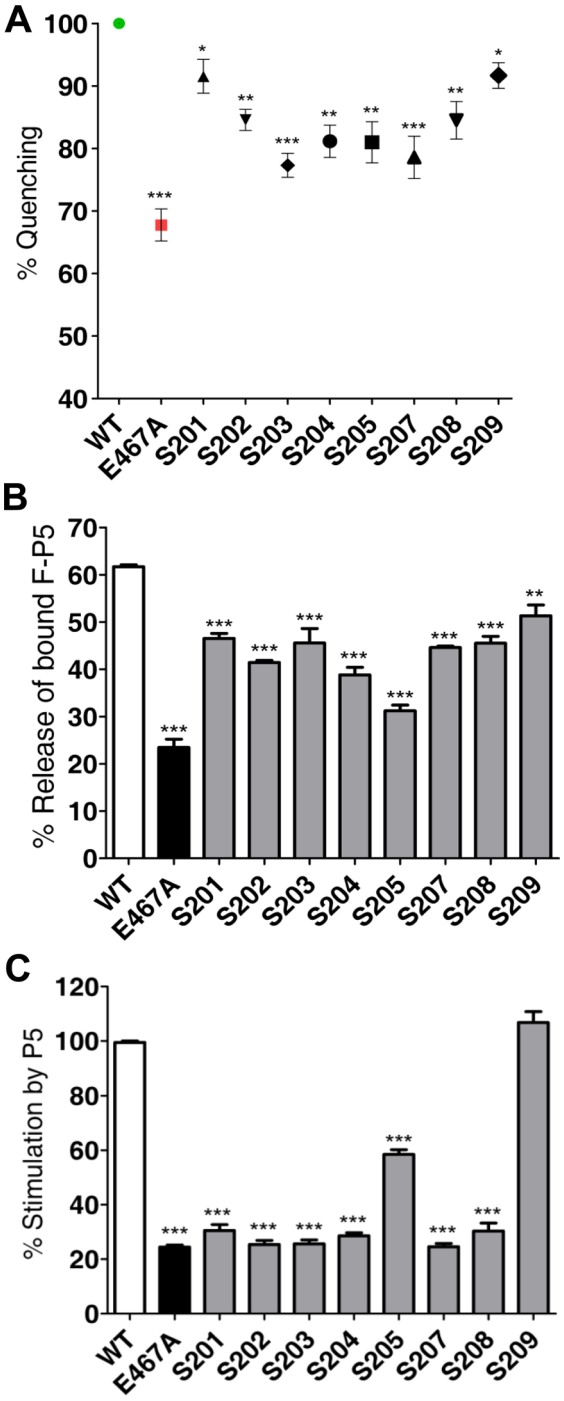

FIGURE 4: Restoration of interdomain communication defects in suppressors. (A) Tryptophan fluorescence quenching analysis. Wild-type, mutant, or suppressor proteins at 2.5 μM were incubated with 2.5 mM ATP at 4°C for 2 min. Decrease in intrinsic tryptophan fluorescence intensity upon ATP binding was measured using a Jasco 6300 spectrofluorometer. Percentage quenching of fluorescence was represented by normalizing the wild-type value as 100%. (B) Determination of ATP-induced substrate release. ATP, 2.5 mM, was added to 5 μM Ssc1[F-P5] complexes of the wild type, mutant, or suppressors, and decrease in anisotropy was monitored. Total percentage decrease in anisotropy values up to 5 min post–ATP addition is represented. (C) Estimation of P5 substrate–mediated stimulation of ATPase activity. The indicated preformed labeled Ssc1[ATP] complexes were subjected to single-turnover ATPase assays in the presence of 100-fold molar excess P5 peptide, as described in *Materials and Methods.* The relative efficiency of stimulation was determined after normalizing the values, setting wild type as 100%.

temperature sensitivity of E467A at 37°C, as shown by drop test analysis on minimal media (Figure 3B). Among these, N508K/T, D519G, and K490R represent four novel suppressor mutations within the *SSC1* gene (Figure 3A).

To demonstrate the mechanism of suppression through intragenic suppressors of E467A, we subjected the individual purified proteins to biochemical analyses. To determine the substrate-binding affinities, we incubated increasing concentrations of each protein with fluorescein-labeled P5 peptide (F-P5) and performed fluorescence anisotropic measurements as reported previously (Pareek *et al.*, 2011). E467A showed ~8.6-fold reduced affinity for the substrate with dissociation constant (K_d) of 1.75 ± 0.269 μM as compared with the wild-type value of 0.20 ± 0.037 μM. Of note, all the suppressors of E467A showed significant reversion in their affinities for peptide binding (Figure 3D and Supplemental Table S2). Furthermore, to understand the kinetics of binding, we measured peptide release rate by displacement of prebound F-P5 by excess unlabeled P5 peptide. The E467A protein showed a slightly elevated rate of dissociation, with k_{off} = 0.0039 ± 0.0001310 s^{-1}, in contrast to the wild-type value of 0.0023 ± 0.0000347 s^{-1} (Supplemental Figure S3 and Supplemental Table S2). In addition, E467A exhibited a lower association rate for peptide binding, with k_{on} = 0.0034 $\mu M^{-1}s^{-1}$ as opposed to 0.014 $\mu M^{-1}s^{-1}$ for the wild type (Supplemental Table S2). The majority of the suppressor proteins showed restoration of substrate affinity by simultaneously altering both dissociation and association rates for peptide binding in comparison to wild type and E467A alone (Supplemental Table S2).

The effect of suppressor mutations on elevated basal ATPase activity of E467A was monitored under single-turnover conditions. Most surprisingly, it was observed that the majority of the suppressors did not significantly reverse the elevated basal ATPase activity of E467A (Figure 3E). Except for suppressors S203 and S209, the basal activities of the suppressors were even further enhanced compared with the E467A mutant alone (Figure 3E). Of interest, the suppressors, except for S209, also demonstrated a strong defect in stimulation of ATPase activity by the J-protein cochaperone Mdj1 in comparison to wild type (Figure 3F). Taken together, our data suggest that the suppressors are capable of correcting a distinct subset of biochemical defects associated with the E467A protein in spite of complete restoration of growth.

Suppression of communication defects from NBD to SBD is sufficient for in vivo functional restoration

To obtain a better understanding of the mechanism of restoration of bidirectional communication by the suppressors, we monitored NBD-to-SBD signal transmission and vice versa by using specific appropriate assays. First, we subjected purified E467A and suppressor proteins to an emission scan between 300 and 400 nm to determine the extent of tryptophan fluorescence quench upon addition of 1000-fold excess ATP. E467A exhibited 30% reduction in quenching in contrast to the wild type (Figures 4A and Supplemental Figure S4), and the majority of the intragenic suppressors showed a significant reversal in this altered property (Figure 4A). Taken together, these observations clearly indicate a defect in allosteric communication from NBD to SBD in the loop mutants, which is significantly alleviated by the suppressors.

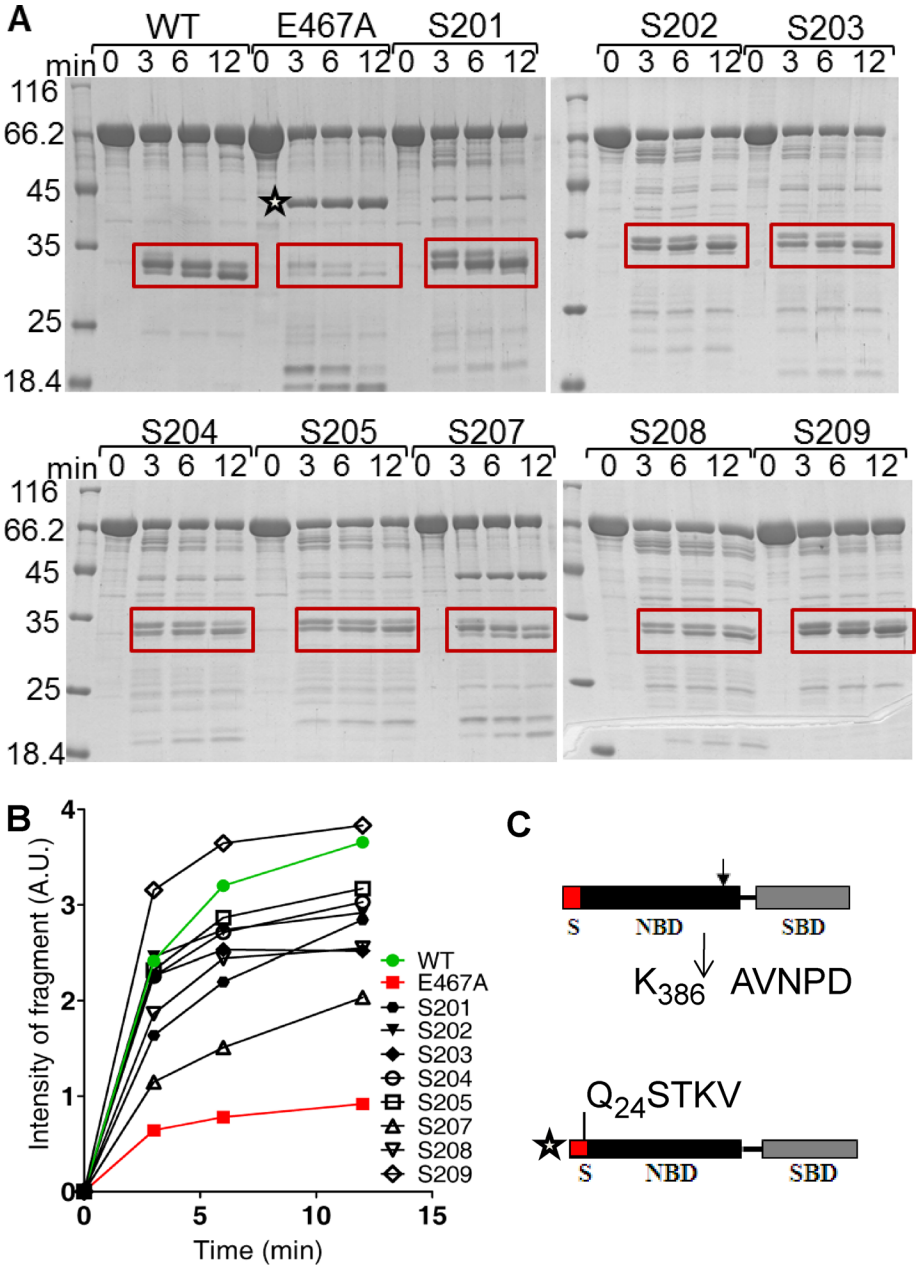

FIGURE 5: Protein conformational differences assessed by proteolytic cleavage analysis. (A) Comparison of trypsin digestion profiles. A limited proteolytic digestion pattern of the wild-type, E467A, and suppressor proteins at different time intervals (in minutes). The major digested fragments (marked within boxes and highlighted by a star) were electroblotted and subjected to N-terminal microsequencing to determine the identity of the fragments. (B) Measurement of the rate of proteolytic cleavage. The major fragments in each case (~30–32 kDa) were quantified densitometrically using Multigauge, version 3.0, software. Total band intensities are plotted as a function of time. (C) Schematic representation of the identities of major fragments as obtained by microsequencing. Top, position of cleavage site leading to generation of the ~30–32 kDa fragments, marked with boxes in A. Bottom, identity of the major ~45-kDa product in E467A, marked with a star in A.

Second, we investigated the ability of the suppressor proteins to release prebound substrate in response to ATP binding. This assay was previously use in *E. coli* DnaK protein to monitor ATP-dependent conformational changes propagated from the NBD to the SBD region (Liberek *et al.*, 1991b; Montgomery *et al.*, 1999). Addition of ATP to a preformed complex of protein[F-P5] leads to dissociation of bound substrate, resulting in observable anisotropy loss, which is used to determine the extent of release. Of interest, the E467A mutant displayed only ~38% substrate release as compared with wild type (Figures 2E and 4B). Of importance, all the suppressors could correct this defect by >50% of substrate release upon ATP binding, further confirming restoration of communication from NBD to SBD as compared with the E467A mutant (Figure 4B).

Finally, we tested the stimulation of basal ATPase activity of each protein by P5 substrate. It is known that substrate binding stimulates the hydrolysis of bound ATP and hence permits the transition of Hsp70 to its ADP-bound, high–substrate affinity form (Jordan and McMacken, 1995; Montgomery *et al.*, 1999). Single-turnover ATPase assays were performed in the presence of 100-fold excess P5, and it was observed that E467A exhibited a dramatic 80% decrease in ATPase stimulation upon substrate binding, indicating interference with conformational signal transmission from the SBD (Figures 2D and 4C). Strikingly, a majority of the suppressors failed to reverse this defect to levels above the E467A mutant alone, although they displayed normal peptide-binding affinity in the ATP-bound state (Figure 4C). Of interest, however, only the S209 suppressor could stimulate ATPase activity similar to wild-type levels. In conclusion, our findings suggest that the suppressors identified are able to restore unidirectional communication at least from the NBD to the SBD in the case of E467A, resulting in the observed functional complementation.

Second-site suppressors result in restoration of conformational changes associated with communication-defective mutations

We hypothesized that the altered biochemical properties are a consequence of conformational modifications caused by the mutations that are suitably reversed in the suppressor proteins. To test this hypothesis, we subjected individual purified proteins to limited proteolytic cleavage using trypsin. This method was previously used to detect the conformational exposure of domain interfaces in Ssc1, as well as in DnaK (Buchberger *et al.*, 1994). Under both ATP- and ADP-bound conditions, wild-type Ssc1 showed a limited proteolysis pattern, leading to formation of stable 30-kDa fragments, which is consistent with previous reports (Pareek *et al.*, 2011). A marked difference from wild type was observed in the cleavage pattern of E467A alone. A time-dependent proteolytic cleavage analysis of the wild-type protein resulted in a stable doublet or triplet of very closely spaced bands, which migrate at a size of 30–32 kDa on SDS–PAGE (Figure 5A). N-terminal sequencing revealed that all three bands had an

identical N-terminus (A_{387}VNPD) located at the terminal end of the NBD just preceding the linker, indicating that the different sizes of the bands are due to differential exposure to a cleavage site at the extreme C-terminal region (Figure 5C, top). However, in the case of E467A, the 30-kDa bands were very unstable and rapidly degraded further into smaller-sized fragments (Figure 5A). Instead, the major stable product of proteolytic cleavage in this case was a 44-kDa fragment, identified as the ATPase domain by N-terminal sequencing (Q_{24}STKV) (Figure 5, A and C, bottom). Of interest, most of the suppressors regained conformational stability and cleavage patterns similar to those of wild type (Figure 5, A and B). Our results show that the E467A mutant possesses a distinct conformational landscape, leading to differential exposure of the linker and SBD regions and hence interfering with its allosteric interfaces. This alteration is suitably reversed by the suppressors, leading to suppression of many of the observed functional defects.

Growth restoration by the suppressors correlates with reversal of defects in protein translocation and mitochondrial biogenesis

The rescue of the temperature-sensitive growth phenotype of the Ssc1 E467A mutant by suppressors is a consequence of restoration of biochemical properties like substrate interactions and protein conformation, making the proteins more responsive to ATP-induced changes required for effective communication. Therefore, to obtain a direct correlation between a role of the loop $L_{4,5}$ in communication and in vivo restoration of functional defects, we tested for protein translocation activity of the mutant and the suppressors. Ssc1 forms the core of the import motor, playing a critical role in importing preproteins destined for the matrix compartment. For this import function, Ssc1 is tethered to the import channel via the peripheral protein Tim44 (Liu *et al.*, 2003). To check whether the mutation altered nucleotide-regulated interactions among import motor components, we performed coimmunoprecipitation (CoIP) studies using mitochondrial lysates. Isolated mitochondria from the respective yeast strains were incubated at a nonpermissive temperature, lysed gently using nonionic detergent in the presence and absence of ATP, and subjected to CoIP using immobilized anti-Ssc1 antibodies. As previously reported, wild-type Ssc1 showed a robust interaction with Tim44 in the absence of ATP, and this binding was sensitive to the presence of ATP (Figure 6A). In contrast, E467A interacted negligibly with Tim44 even in the absence of ATP (Figure 6A). Of interest, most of the suppressors of E467A could restore interaction with Tim44 in the nucleotide-free form but exhibited sensitivity in the presence of ATP, similar to wild type (Figure 6A). In agreement with previous reports, these results imply that restoration of allosteric communication by the suppressors also recovers the ability to undertake nucleotide-regulated interactions required for in vivo functions such as import (Becker *et al.*, 2009).

To determine whether the compromised interaction of Ssc1 with the translocation channel affects protein import, we analyzed the efficiency of precursor processing in the mutant and its suppressors. Using an in vivo precursor accumulation assay, we monitored the cytosolic accumulation of unprocessed mitochondrial proteins such as Hsp60 as a consequence of compromised Ssc1 activity during translocation (Davis *et al.*, 1999). After growth under permissive conditions, the yeast strains were shifted to nonpermissive temperatures to induce the phenotype, and the cell lysates were subsequently analyzed for the presence of precursor forms of Hsp60, an abundant matrix-localized protein. The E467A strain showed significant levels of Hsp60 precursor form as compared with wild type, indicating compromised import function (Figure 6B). Remarkably, however, the suppressors could robustly suppress this import defect, as none of them showed any consequential accumulation of precursor proteins in comparison to mutant alone (Figure 6B). Moreover, the mutant showed impairment in translocation rate, as found by measuring the kinetics of protein import into isolated mitochondria, using a purified precursor protein, $Cytb_2(47)$– dihydrofolate reductase (DHFR; Figure 6, C and D). In agreement with the precursor accumulation assay, most of the suppressors demonstrated restoration in the rate of precursor translocation into mitochondria (Figure 6, C and D).

In addition to the import and folding functions, Ssc1 also plays a critical role in the biogenesis of mitochondria. To determine any differences in mitochondrial content due to the mutations, we performed staining by 10-*N*-nonyl acridine orange, which specifically binds to the cardiolipin component of mitochondrial membrane, providing an estimate of total mitochondrial mass. We observed that the E467A strain had 30% reduction in mitochondrial mass in comparison to wild type (Figure 6E). On the other hand, most of the suppressor strains exhibited significantly higher mitochondrial mass contents than E467A alone and very much comparable to the wild type (Figure 6E). Thus overall our results show that the E467A mutation leads to several in vivo functional defects related to mitochondrial processes, which are substantially reversed by the suppressors, thereby restoring the growth of the strains.

The loop $L_{4,5}$ modulates interdomain communication through the linker region

The highly conserved linker region plays the pivotal role of connecting the NBD and the SBD in Hsp70s and is intrinsically involved in the domain communication process. Both the hydrophobic and charged residues of the linker have been shown to be critical for relative positioning of the domains (Swain *et al.*, 2007), modulation of allosteric communication (Vogel *et al.*, 2006b), and chaperoning activity in DnaK (Han and Christen, 2001). In addition, E467A and its suppressors showed a differential exposure of the extreme C-terminal of the NBD, immediately preceding the linker region. Therefore, to test the possibility that the loop $L_{4,5}$ regulates communication by altering the domain interface via linker region, we mutated the conserved negatively charged aspartate residues of the linker alone and in combination with E467A mutant. Substitution of Asp with Arg at the linker 411 position (D411R) did not result in a growth defect (Figure 7A). However, the D411R mutant protein exhibited a twofold increase in basal ATPase activity (Figure 7D), indicative of mild impairment in interdomain communication. This domain communication–defective nature of D411R was further corroborated by modest reductions in stimulation of ATPase activity by substrate (Figure 7E), extent of substrate release (Figure 7F), and degree of tryptophan fluorescence quenching upon ATP binding (Figure 7G). Of interest, in contrast, the mutation of the Asp residue at position 416 of the linker region to Arg (D416R) yielded a severe growth defect, as evidenced by its inviability on 5-FOA medium (Figure 7B). The D416R protein showed a 4.5-fold increase in basal ATPase activity (Figure 7D), which was stimulated fivefold less by P5 as compared with the wild-type protein (Figure 7E). Furthermore, upon addition of ATP, the protein displayed very low peptide release (<10%; Figure 7F) and significantly lowered quenching of tryptophan fluorescence (Figure 7G) in comparison to wild type. Together these results suggest that, similar to the analogous residue in DnaK (Vogel *et al.*, 2006b), the aspartate residue at position 416 is extremely crucial for the conformational transitions required for allosteric communication.

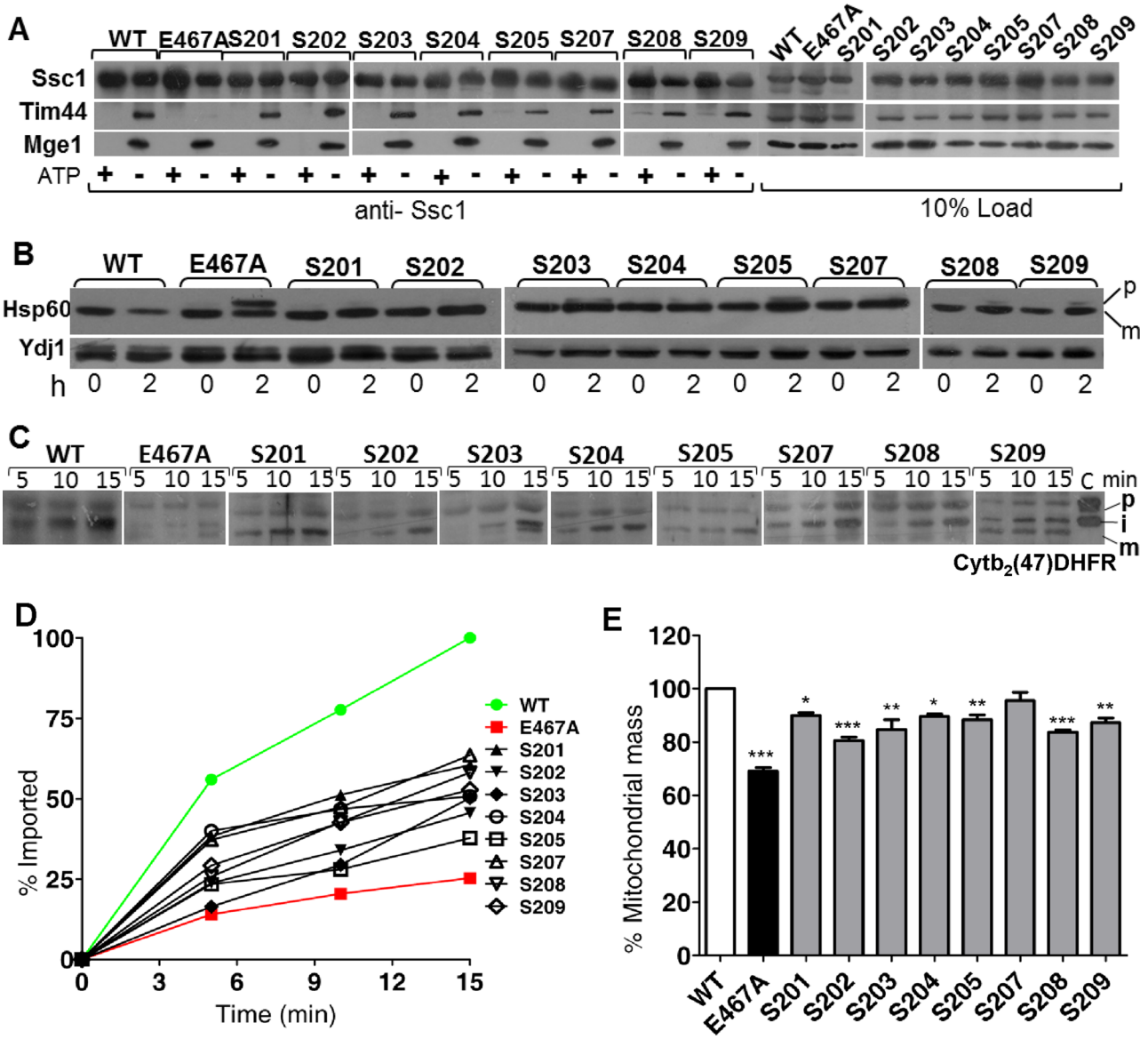

FIGURE 6: Effects of E467A and suppressor mutations on protein translocation and mitochondrial biogenesis. (A) Interaction of Ssc1 with Tim44 by coimmunoprecipitation. Purified mitochondrial lysates were subjected to immunoprecipitation by Ssc1-specific antibodies in the presence (+) and absence (–) of 1 mM ATP as described in *Materials and Methods*. Interaction with Mge1 and Tim44 was detected by using specific antibodies. Ten percent of untreated mitochondrial lysate in each case was loaded as control. (B) Precursor accumulation analysis. Whole-cell extracts were prepared from each strain as indicated before and after heat shock for 2 h and subjected to immunoblotting against Hsp60 to detect the relative levels of its precursor (p) and mature (m) forms. The cytosolic protein Ydj1 was used as a loading control. (C) Determination of in vitro import kinetics. The time-dependent import of $Cytb_2(47)$-DHFR into purified mitochondria was performed, and import was monitored by immunoblotting using a DHFR-specific antibody. One hundred percent precursor protein offered to the mitochondria was loaded as control (c); p, i, and m, precursor, intermediate, and mature forms of $Cytb_2(47)$-DHFR, respectively. (D) The amount of intermediate form imported was quantified and plotted as a function of time, setting the maximum import by wild type as 100%. (E) Mitochondrial mass estimation. From each strain, 0.2 OD cells at A_{600} were stained with 10-*N*-nonyl acridine orange (NAO) and subjected to flow cytometry. The mean fluorescence intensity value of 10,000 events in each case was used to determine the overall mitochondrial mass and represented by normalizing the values setting wild type as 100%.

To determine whether there is a synergistic effect of the loop $L_{4,5}$ with the linker region on domain communication, we generated combined mutations between E467A and D411R. Strikingly, although D411R is completely viable, the combination E467A-D411R was found to be lethal, as demonstrated by lack of growth on 5-FOA (Figure 7B). On the other hand, D416R is inviable, but in combination, E467A-D416R showed a semidominant phenotype indicative of a mutual interplay and additive effect between the linker and the loop $L_{4,5}$ (Figure 7, B and C). This was further verified by biochemical analysis with the purified mutant proteins using assays specific for domain communication. We found that the E467A-D411R mutant combination resulted in 3.8-fold elevated basal ATPase rate (Figure 7D) and also severely impaired stimulation by substrate (Figure 7E) as compared with the respective single mutations. Further, the

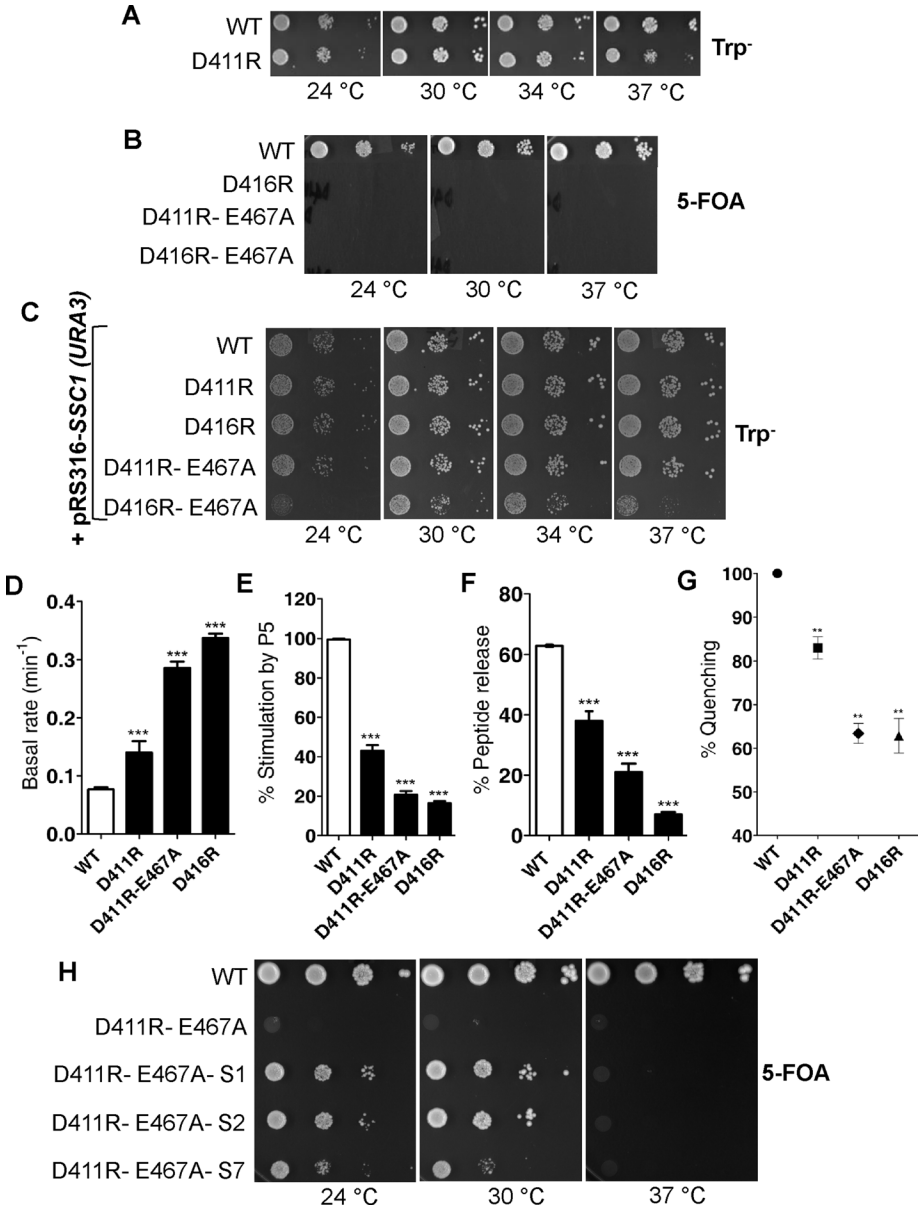

FIGURE 7: Effects of alterations in charged residues from the linker region in modulating interdomain communication. (A–C) Growth phenotype analysis. (A) Spot analysis of serially diluted cells expressing pRS314-*ssc1*$_{D411R}$ on minimal medium incubated at indicated temperatures for 65 h. (B) Yeast cells harboring the D416R, D411R-E467A, and D416R-E467A mutations were serially diluted and subjected to spot analysis on minimal medium containing 5-FOA and incubated for 96 h at the indicated temperatures. (C) Similarly, yeast strains expressing the aforementioned mutations in the presence of the wild-type *SSC1* copy on pRS316 plasmid were subjected to spot analysis on minimal media. The plates were incubated at various temperatures up to 45 h to demonstrate the semidominant phenotype. (D) Determination of basal ATPase activity. Basal ATPase activities of the indicated proteins were determined by single-turnover ATPase assays using preformed labeled Ssc1[ATP] complexes. (E) Estimation of ATPase stimulation by P5 peptide. The efficiency of stimulation of basal ATPase activities was determined in the presence of 100-fold molar excess of P5 substrate. The relative efficiency of stimulation was represented after normalizing the values of wild type as 100%. (F) Measurement of extent of ATP-induced peptide release by fluorescence anisotropy. ATP, 2.5 mM, was added to 5 μM wild-type or mutant Ssc1[F-P5] complexes, and the decrease in anisotropy was monitored. The total percentage decrease in anisotropy 5 min post–ATP addition is represented. (G) Tryptophan fluorescence quenching assay. The tryptophan fluorescence quenching of indicated proteins upon addition of 1000-fold excess ATP was determined, and the percentage decrease in fluorescence intensity is represented by normalizing the wild-type value as 100%. (H) Effect of suppressors on the growth phenotype of D411R-E467A mutation. Cells equivalent to 1 OD at A_{600} of the respective yeast strains were subjected to serial dilution and spotted on minimal medium containing 5-FOA. The plates were incubated for 96 h at the indicated temperatures for phenotype analysis.

protein was markedly compromised in ATP-dependent conformational changes required for release of bound substrate and quenching of fluorescence (Figure 7, F and G), together indicating significant impairment in allosteric communication.

Having established the combined role of the linker and loop $L_{4,5}$ in modulating interdomain communication, we tested for the ability of some of the suppressors in rescuing the observed defects. For this purpose, one representative suppressor from each residue (i.e., S1-D519E, S2-V524I, and S7-N508T) was subcloned into the E467A-D411R backbone. Strikingly, the resulting yeast strains showed significant growth rescue of the E467A-D411R–associated lethality at different temperatures on 5-FOA medium (Figure 7H). Together our data suggest that the linker and loop $L_{4,5}$ play a synergistic role in regulating interdomain communication, and the novel suppressors identified can suppress the allosteric defects from distinct regions of the protein.

DISCUSSION

The present study demonstrates the critical role of interdomain communication in mtHsp70s, which are essential for a battery of in vivo functions in eukaryotic systems. Although the importance of domain communication in Hsp70s is well understood in the prokaryotic context, relevant mechanistic insight into allosteric regulation governing mtHsp70s is elusive. Using *S. cerevisiae* Ssc1 as a model system, we uncovered structural elements within mtHsp70s that are required for allosteric modulation of the chaperone cycle, thereby controlling multiple physiological functions, including import and folding of hundreds of mitochondrial matrix- targeted proteins.

Residues from SBD loop $L_{4,5}$ are involved in interdomain communication in mtHsp70s.

Our genetic and biochemical data provide compelling evidence to indicate the involvement of a loop $L_{4,5}$, in the modulation of allostery between the NBD and the SBD of mtHsp70s. Amino acid substitutions within this loop in Ssc1 impart lethal or temperature-sensitive phenotypes, thus showing its significance in governing Ssc1's cellular functions. Biochemical analyses indicate that there is a direct correlation between the

extent of impairment in domain communication and the threshold limit to retain in vivo functions required for cell viability. Of interest, all three mutants from the loop $L_{4,5}$, namely Q465A, G466E, and E467A display differential growth sensitivity. The compromised growth of mutants is a consequence of strong impairment in allosteric regulation. Our experiments show that the mutants exhibit significant defects in extent of bound-peptide release upon binding of ATP at the NBD and in peptide-induced ATPase stimulations, which are key hallmarks of bidirectional interdomain communication. We predict that this is due to loss of allosteric coupling between NBD and SBD through the linker region, which is known to play a critical role in maintaining an allosteric interface (Vogel *et al.*, 2006b). In addition, all three mutants exhibit higher levels of elevated basal ATPase activity, which is one of the key features associated with a disrupted interdomain interface modulated via the linker region (Montgomery *et al.*, 1999). The limited proteolysis analysis provides additional evidence that the E467A mutant has a relatively greater exposure of the C-terminal of the NBD preceding the linker region, thereby altering the interdomain interface and leading to loss of allosteric regulation.

In agreement with our experimental findings, a recent crystal structure of DnaK in its ATP-bound state provides key insights into the NBD–SBD contacts in the docked state (Kityk *et al.*, 2012). Significantly, the corresponding loop $L_{4,5}$ has been identified in DnaK as an important contact site of the NBD–SBDβ interface (β-interface) mediating the allostery (Kityk *et al.*, 2012; Qi *et al.*, 2013). Moreover, in *E. coli* DnaK, a glutamine residue of the loop $L_{4,5}$ at position 442 (Q442) is involved in hydrogen bonding with Arg-151 and Asp-148 on the NBD in the ATP-bound state (Qi *et al.*, 2013). Strikingly, mutation at the corresponding $L_{4,5}$ residue, Q465 in yeast Ssc1 to alanine (Q465A), leads to compromised growth with domain communication defects, thus further strengthening the involvement of the loop. The amino acid sequence in the loop $L_{4,5}$ is conserved in Hsp70s, including mtHsp70s across species. The human mtHsp70$_{G489E}$, associated with myelodysplastic syndrome, showed complete loss of domain communication, leading to impairment in chaperone function (Goswami *et al.*, 2010), and the corresponding mutation in yeast Ssc1, G466E, exhibited a severe defect in allosteric regulation, leading to inviability. The other analogous mutations within the human mtHsp70 loop $L_{4,5}$ namely Q488A and E490A, also displayed impaired allosteric coupling between the NBD and the SBD, resulting in loss of bidirectional communication. Overall, our results provide the first experimental evidence on the relative importance of the loop $L_{4,5}$ residues in eukaryotic mtHsp70s across species for the maintenance of a proper allosteric interface required for conformational transitions between the SBD and the NBD critical for in vivo chaperone function.

Intragenic suppressors shed light on in vivo functional regulation of mtHsp70 proteins

The conditional mutant E467A showed a distinct conformational change, thus disrupting the allosteric interface between the SBD and the NBD by partially exposing the linker region. Strikingly, the intragenic suppressors within the SBD, generated through an unbiased genetic screen against E467A, exhibit a remarkable ability to restore the growth phenotype of the mutant. In addition, the suppressors could partially restore the altered interdomain interface required for allosteric signaling via the linker region. Surprisingly, although the suppressors were able to restore a majority of the in vivo functions, a few basic intrinsic properties associated with E467A remained unchanged at the biochemical level. These include high ATPase activity and loss of both Mdj1- and peptide-mediated stimulation of ATPase activity. This suggests that communication from the SBD to the NBD is not restored in most suppressors, except for S209.

Recent nuclear magnetic resonance (NMR) mapping experiments showed that there exist two interdomain interfaces, namely NBD-SBDβ (β-interface) and SBDβ-SBDα (α-interface), with opposing energetics that regulate allosteric communication in bacterial DnaK (Zhuravleva *et al.*, 2012). Intriguingly, both the E467A mutant and the suppressors S201–S208 originate from the same proposed β-interface. Therefore it is conceivable that the suppressors S201–S208 could nullify the effect of mutation within the same interface conformationally by mediating through the linker region. This results in partial one-way correction of communication from NBD to SBD, thus suppressing the in vivo defects, although it is also likely possible that the mutant and suppressors may exist in the ensemble of conformations mimicking the Hsp40-coupled state. As a result, they are able to intrinsically hydrolyze ATP at a rate that is sufficiently high to drive the ATPase cycle, and hence their dependence on J-protein cochaperone stimulation may have been abolished. In parallel, reversal of the peptide-binding defects of E467A at the SBD may be crucial for in vivo functional restoration, leading to suppression of phenotypes such as import and folding defects, thus driving the functional chaperone cycle, in combination with enhanced basal ATPase activity. The most intriguing aspect of the suppressors S201–S208 is the fact that restoration of allosteric signaling in one direction alone is sufficient to reverse in vivo functional ability, including growth phenotype, raising the interesting possibility that signal transmission from the NBD to the SBD is a more critical event of the allosteric process, which is bidirectional in nature.

On the other hand, the novel suppressor S209 showed remarkable recovery of the interdomain communication defects of the mutant E467A. Of interest, S209 originates from the α-interface and therefore nullifies the effect of the opposing β-interface, thereby suppressing the communication defects of the original mutation in both directions. Unlike the suppressors S201–S208, S209 is able to suppress the elevated basal activity of the mutant as well as augment peptide-mediated ATPase stimulation, suggesting that the α-interface plays a critical modulatory role in SBD-to-NBD allosteric signaling.

The linker plays a synergistic role with the residues of loop $L_{4,5}$ in allosteric signaling

The conserved linker region connecting the two domains in Hsp70s was previously reported to play an important role in the communication process (Vogel *et al.*, 2006b; Swain *et al.*, 2007). Our results corroborate the previous findings and reveal that the D416 residue plays an indispensable role in mediating the allosteric cascades between SBD and NBD. At the same time, D411 and D416 linker residues interplay in a synergistic role with the loop $L_{4,5}$ in conformationally reorganizing the interdomain interface that regulates bidirectional communication between SBD and NBD. Therefore the combined mutations between linker and loop $L_{4,5}$ residues lead to complete disruption of the allosteric effect, thereby causing a strong synthetic lethal phenotype. Based on crystal structure information, it is reasonable to believe that the interaction of loop $L_{4,5}$ with the NBD is directly regulated through the linker region by maintenance of an optimum distance between the interacting regions governing the β-interface. As a result, the suppressors isolated within the β-interface could suppress the interdomain communication defects by relatively altering the conformational positioning of the linker region, regaining the allosteric signaling between domains and restoring in vivo functional defects.

In summary, our results reveal for the first time the in vivo significance of the loop $L_{4,5}$ in eukaryotic mtHsp70s for domain communication and its possible role in protein translocation into mitochondria. The novel class of suppressors identified provides compelling evidence of the unique mechanisms governing the restoration of functional defects of the mutants, further strengthening our understanding of allosteric regulation in mtHsp70s across species, and at the in vivo level.

MATERIALS AND METHODS

Plasmid construction, yeast strains, and genetic analysis

The *ssc1*Δ haploid yeast strain (*trp1–1 ura3–1 leu2–3, 112his3–11, 15 ade2–1 can1–100 GAL2+ met2-Δ1 lys2-Δ2ssc1ΔCla*I::LEU2) containing the plasmid *pRS316:SSC1(URA3)* was used for in vivo analyses. The strain was transformed with the *SSC1* gene (wild type, mutants, or suppressors) cloned under its native promoter using the centromeric vector pRS314 and selected on tryptophan dropout plates. The transformed strains were subjected to plasmid shuffling on 5-FOA (US Biological Life Sciences, Salem, MA) medium to eliminate the *pRS316:SSC1(URA3)* plasmid. Viable strains were recovered on rich medium (yeast/peptone/dextrose [YPD]) and subjected to spot analysis on minimal (tryptophan dropout) medium. In the case of lethal mutations, the transformed strains were subjected to spot analysis on 5-FOA–containing medium to demonstrate the lethal phenotype.

The mutations in *SSC1* and human mtHsp70 coding sequences were generated by PCR-based QuikChange site-directed mutagenesis, using high-fidelity Pfu Turbo DNA Polymerase (Stratagene, La Jolla, CA). The mutations were verified by plasmid sequencing at Eurofins (Bangalore, India). For protein purification using the bacterial expression system, the histidine-tagged open reading frames (devoid of mitochondrial targeting sequence) of human mtHsp70 (Goswami *et al.*, 2010) and Ssc1 (Pareek *et al.*, 2011) were cloned in pRSFDuet-1vector along with the yeast Zim17 as previously described. The mutant and suppressors were subcloned into pRSFDuet-1-*SSC1* construct, using internal restriction sites *Spe*I and *Msc*I.

To obtain intragenic suppressor mutations, we generated a library of random mutations through PCR amplification of the coding region corresponding to *SSC1* SBD fragment containing the E467A mutation by forward (5′ GAGGTTACTGACGTCTTATTATTAG 3′) and reverse (5′ GTATCGTTGGCCAATTGGTCAGCCTT 3′) primers using low-fidelity *Taq* DNA polymerase, as described previously (Cirino *et al.*, 2003; McCullum *et al.*, 2010; Pareek *et al.*, 2013). This randomly mutagenized PCR fragment (nucleotide positions, +1248 to +1732), after digestion with *Aat*II/*Mfe*I restriction enzymes, was subcloned into a modified pRS314-*SSC1* vector (deleted for additional *Mfe*1 site from the vector backbone) using the same restriction sites, thereby encoding the full-length protein containing the mutations. The *ssc1*Δ haploid yeast strain was transformed with the suppressor library and incubated at 30°C on tryptophan-lacking medium. The transformants were patched onto 5-FOA plates to select candidates that could grow in the absence of the wild-type copy (pRS316 plasmid). The candidates were replicated on tryptophan dropout plates and incubated at 34 and 37°C to score the suppression phenotypes. Plasmids were rescued from suppressor mutants by previously described protocols (Robzyk and Kassir, 1992; Pareek *et al.*, 2013) and subsequently sequenced to identify the positions of the mutated nucleotides.

Protein purification and partial proteolytic cleavage

The purification of human and yeast hexahistidine-tagged proteins was carried out by coexpression with yeast Zim17 protein in *E. coli* BL21 (DE3) using similar protocols as previously described (Goswami *et al.*, 2012). Briefly, the cultures were grown at 30°C (or 25°C, in the case of temperature-sensitive mutants) to an $A_{600} = 0.5$, followed by induction of protein expression for 6 h, using 1 mM isopropyl 1-thio-β-D-galactopyranoside (IPTG). The cells were harvested and lysed in buffer C (20 mM 4-(2-hydroxyethyl)-1-piperazineethanesulfonic acid [HEPES]-KOH, pH 7.5, 150 mM KCl, 20 mM imidazole, and 10% glycerol) containing 2.5 mM magnesium acetate and 0.2 mg/ml lysozyme and protease inhibitor mixture, followed by incubation at 4°C for 1 h. The samples were then treated with 0.2% deoxycholate for 30 min at 4°C and subjected to sonication at 28% amplitude, five times (15 s each), with intervals of 2 min on ice. The resultant lysates were clarified by centrifugation at 40,000 × *g* for 30 min at 4°C. The soluble supernatant was incubated with nickel-nitriloacetic acid–Sepharose (GE Healthcare, Buckinghamshire, United Kingdom) for 2 h at 4°C to allow binding. Unbound proteins and nonspecific contaminants were removed by two washes of buffer C alone, followed by five washes of 0.05% Triton X-100 contained in buffer C, to remove Zim17 protein bound to Ssc1. Subsequently, sequential single washes were carried out with 1 mM ATP, 1 M KCl, and 40 mM imidazole, respectively, each contained in buffer C. The proteins were eluted with buffer C containing 250 mM imidazole and subjected to step dialysis to remove imidazole. Purity >95% was obtained for all the protein by this method.

For partial proteolytic cleavage by trypsin, 20 μg of protein was incubated in buffer A (25 mM HEPES-KOH, pH 7.5, 100 mM KCl, and 10 mM $Mg(OAc)_2$) containing 5 mM ATP for 10 min at 25°C, and proteolysis was initiated by addition of 0.2 μg (1:100 [wt/wt]) trypsin (type 1, from bovine pancreas). At the indicated time points, aliquots of the reaction mix corresponding to 5 μg of protein were removed, and the reaction was stopped using phenylmethylsulfonyl fluoride (PMSF). The samples were resolved by SDS–PAGE, followed by Coomassie dye staining. Protein, 5 μg, was loaded as precleavage control in each case. For microsequencing, the cleavage products were electroblotted on polyvinylidene fluoride membrane using 10 mM *N*-cyclohexyl-3-aminopropanesulfonic (CAPS) acid buffer and stained using Ponceau S. The fragments were excised and subjected to N-terminal sequencing using a Procise protein sequencer from Applied Biosystems.

Fluorescence anisotropy–based peptide-binding analysis

Substrate interaction studies were performed using F-P5 having the sequence CALLLSAPRR, as described previously (Liu *et al.*, 2001; Pareek *et al.*, 2011). Briefly, increasing concentrations of the proteins were incubated with 25 nM F-P5 in buffer A for 1 h at 25°C for equilibrium binding. Anisotropy measurements were recorded on a Beacon-2000 fluorescence polarization system (Panvera, Madison, WI) using excitation at 490 nm and emission at 535 nm. Anisotropy values were fitted to a one-site binding hyperbola equation to calculate the equilibrium dissociation constant (K_d). For analyzing substrate dissociation rates, 1000-fold excess of unlabeled P5 peptide was added to human mtHsp70 or Ssc1 protein[F-P5] complexes at equilibrium, and anisotropy values were recorded every 6 s. A one-phase exponential decay equation was used to calculate the k_{off} values. In the case of on-rate determination, the increase in anisotropy was monitored at intervals of 6 s after addition of 25 nM F-P5 peptide to 5 μM protein and analyzed using a one-phase exponential association equation. To calculate percentage release of bound substrate by ATP, the wild-type or mutant proteins were incubated with F-P5 in the absence of nucleotides for 1 h at 25°C. After substrate binding reached equilibrium, the saturated values were set as

100% (in the absence of nucleotide) to calculate the percentage loss in fluorescence anisotropy of bound substrate upon ATP addition up to 5 min postaddition. All data for substrate interactions were analyzed using Prism 5.0 (GraphPad).

Single-turnover ATPase assays

Labeled human mtHsp70/Ssc1[ATP] complexes were prepared by incubating 100 µg of individual purified proteins with 50 µM ATP and 25 µCi of [γ-^{32}P]ATP in buffer A on ice for 30 s (in the case of Ssc1 proteins) or 3 min (in the case of human mtHsp70 proteins). The complexes (containing 1 µM protein) were immediately isolated on Sephadex G50 NICK columns (GE Healthcare) and frozen in liquid nitrogen. Single-turnover assays with the preformed complexes were performed in buffer A at 25°C either in buffer alone (basal) or in the presence of desired ratios of P5 substrate or Mdj1 protein. The reaction was terminated at different time intervals and separated by TLC on PEI-cellulose matrix (Macherey-Nagel). The percentage conversion of ATP to P_i at each time point was fitted to a one-phase exponential binding equation using Prism 5.0 to determine the rate of hydrolysis. The efficiency of stimulation by P5 or Mdj1 was calculated from the fold increase in rate of hydrolysis over the basal rate and represented by normalizing the fold increase of wild type as 100%.

Precursor processing and in vitro import analysis

For estimation of precursor processing efficiency, the yeast strains were grown at 28°C in YPD medium to early log phase. The cultures were then shifted to the nonpermissive temperature of 37°C for 2 h to induce the temperature-sensitive phenotype. Cells equivalent to an OD of 2 at A_{600} each from before and after the temperature shift were lysed using 0.1 N NaOH and resuspended in SDS sample buffer, and the whole-cell extracts were separated by SDS–PAGE. Immunoblot analysis was performed using an antibody against Hsp60 protein.

For analysis of in vitro import kinetics, mitochondria were isolated from all strains under permissive growth conditions. Purified mitochondria, 200 µg, from each strain was preincubated in import buffer (50 mM 3-(*N*-morpholino)propanesulfonic acid [MOPS]-KOH, pH 7.2, 500 mM sorbitol, 80 mM KCl, 10 mM $Mg(OAc)_2$, 2 mM KH_2PO_4, 1 mM $MnCl_2$, and 2% bovine serum albumin) at the nonpermissive temperature of 37°C for 15 min. Import was initiated by addition of a saturating amount of purified $Cytb_2$(47)-DHFR precursor protein in the presence of 8 mM each ATP and NADH, and the reaction was stopped at indicated time points using valinomycin, followed by treatment with proteinase K to remove the fraction of recombinant DHFR protein not imported into mitochondria. Finally, the proteinase K treatment was terminated by PMSF, and the pellets obtained by centrifugation were washed in SM-KCl buffer (600 mM sorbitol, 20 mM MOPS-KOH, pH 7.2, 80 mM KCl). The mitochondrial pellet was resuspended in SDS sample buffer and analyzed by SDS–PAGE and immunoblotting using an antibody against DHFR.

Coimmunoprecipitation analysis

Purified mitochondria, 300 µg, were incubated in immunoprecipitation (IP) buffer (250 mM sucrose, 80 mM KCl, 20 mM MOPS-KOH, pH 7.2, 0.2% Triton X-100, 1 mM PMSF) in the presence (1 mM ATP and 10 mM $Mg(OAc)_2$ added) or absence (5 mM EDTA added) of ATP on ice for 30 min for lysis. After centrifugation at 16,000 × *g* and 4°C for 10 min, the resultant lysates were added to protein A–Sepharose beads cross-linked with antibody against Ssc1. The lysates were allowed to interact with the beads for 2 h on a nutating mixer at 4°C, following which they were washed three times in IP buffer. Finally, the beads were resuspended in 2× SDS sample buffer and boiled at 90°C for 2 min. The total supernatant was loaded for SDS–PAGE, followed by electroblotting and immunodecoration with antibodies against Mge1, Tim44, and Ssc1 to detect interaction under the different nucleotide conditions.

Statistical analysis

The error bars in the bar charts represent the SEM and are derived from a minimum of two replicates. Significance testing (in comparison to wild-type values) was performed by one-way analysis of variance with Dunnett's multiple comparison post test using the Prism 5.0 software. Asterisks denote significance: *$p \leq 0.05$; **$p \leq 0.01$; ***$p \leq 0.001$.

Miscellaneous

Yeast mitochondria isolation (Daum *et al.*, 1982), tryptophan fluorescence quenching (Pareek *et al.*, 2011), and flow cytometry analysis for mitochondrial mass estimation (Goswami *et al.*, 2012) were performed using standard protocols, unless specified. Multiple sequence alignment was performed using the ClustalW2 online tool (European Molecular Biology Laboratory, European Bioinformatics Institute, www.ebi.ac.uk/Tools/msa/clustalw2/). Homology modeling of the ADP states of Ssc1 and human mtHsp70 was carried out using the ESyPred3D Web Server 1.0 (www.unamur.be/sciences/biologie/urbm/bioinfo/esypred/) with bacterial DnaK (2KHO) as a template. For modeling the ATP-state of Ssc1, the DnaK template 4JN4 was used in the Swiss Model online server (http://swissmodel.expasy.org/). The antibodies against Hsp60, Mge1, Tim44, and Ydj1 were gifts from E. A. Craig's laboratory, and the antibodies against DHFR and Ssc1 were generated by injection of purified protein into rabbits (IMGENEX India, Bhubaneshwar, India). Immunoblot analysis was performed by the ECL system (PerkinElmer, Waltham, MA) according to manufacturer's instructions. All fine chemicals used for experiments were obtained from Sigma-Aldrich, unless otherwise specified.

ACKNOWLEDGMENTS

The haploid yeast strain and yeast protein-specific antibodies were kind gifts from Elizabeth A Craig (University of Wisconsin–Madison, Madison, WI). We thank the Flow Cytometry facility of the Indian Institute of Science (Bangalore, India), the Protein Sequencing facility of the Department of Biochemistry, and Lakshmi Prasanna Darbha for technical assistance. This work was supported by a Lady Tata Memorial Trust Young Researcher Award Grant (LTMT 0005). We acknowledge a Swarnajayanti Fellowship from the Department of Science and Technology, India (to P.D.S.), and the Council of Scientific and Industrial Research, India, for Senior Research Fellowships (to M.S. and A.V.G.).

REFERENCES

Becker D, Krayl M, Strub A, Li Y, Mayer MP, Voos W (2009). Impaired interdomain communication in mitochondrial Hsp70 results in the loss of inward-directed translocation force. J Biol Chem 284, 2934–2946.

Bertelsen EB, Chang L, Gestwicki JE, Zuiderweg ER (2009). Solution conformation of wild-type E. coli Hsp70 (DnaK) chaperone complexed with ADP and substrate. Proc Natl Acad Sci USA 106, 8471–8476.

Bhattacharya A, Kurochkin AV, Yip GN, Zhang Y, Bertelsen EB, Zuiderweg ER (2009). Allostery in Hsp70 chaperones is transduced by subdomain rotations. J Mol Biol 388, 475–490.

Blamowska M, Sichting M, Mapa K, Mokranjac D, Neupert W, Hell K (2010). ATPase domain and interdomain linker play a key role in aggregation of mitochondrial Hsp70 chaperone Ssc1. J Biol Chem 285, 4423–4431.

Buchberger A, Theyssen H, Schroder H, McCarty JS, Virgallita G, Milkereit P, Reinstein J, Bukau B (1995). Nucleotide-induced conformational

changes in the ATPase and substrate binding domains of the DnaK chaperone provide evidence for interdomain communication. J Biol Chem 270, 16903–16910.
Buchberger A, Valencia A, McMacken R, Sander C, Bukau B (1994). The chaperone function of DnaK requires the coupling of ATPase activity with substrate binding through residue E171. EMBO J 13, 1687–1695.
Cirino PC, Mayer KM, Umeno D (2003). Generating mutant libraries using error-prone PCR. Methods Mol Biol 231, 3–9.
Craig EA, Marszalek J (2002). A specialized mitochondrial molecular chaperone system: A role in formation of Fe/S centers. Cell Mol Life Sci 59, 1658–1665.
Craven SE, French D, Ye W, de Sauvage F, Rosenthal A (2005). Loss of Hspa9b in zebrafish recapitulates the ineffective hematopoiesis of the myelodysplastic syndrome. Blood 105, 3528–3534.
Daum G, Bohni PC, Schatz G (1982). Import of proteins into mitochondria. Cytochrome b2 and cytochrome c peroxidase are located in the intermembrane space of yeast mitochondria. J Biol Chem 257, 13028–13033.
Davis JE, Voisine C, Craig EA (1999). Intragenic suppressors of Hsp70 mutants: interplay between the ATPase- and peptide-binding domains. Proc Natl Acad Sci USA 96, 9269–9276.
D'Silva PR, Schilke B, Hayashi M, Craig EA (2008). Interaction of the J-protein heterodimer Pam18/Pam16 of the mitochondrial import motor with the translocon of the inner membrane. Mol Biol Cell 19, 424–432.
D'Silva PR, Schilke B, Walter W, Craig EA (2005). Role of Pam16's degenerate J domain in protein import across the mitochondrial inner membrane. Proc Natl Acad Sci USA 102, 12419–12424.
Geissler A, Krimmer T, Bomer U, Guiard B, Rassow J, Pfanner N (2000). Membrane potential-driven protein import into mitochondria—the sorting sequence cytochrome b(2) modulates the delta psi-dependence of translocation of the matrix-targeting sequence. Mol Biol Cell 11, 3977–3991.
Goswami AV, Chittoor B, D'Silva P (2010). Understanding the functional interplay between mammalian mitochondrial Hsp70 chaperone machine components. J Biol Chem 285, 19472–19482.
Goswami AV, Samaddar M, Sinha D, Purushotham J, D'Silva P (2012). Enhanced J-protein interaction and compromised protein stability of mtHsp70 variants lead to mitochondrial dysfunction in Parkinson's disease. Hum Mol Genet 21, 3317–3332.
Han W, Christen P (2001). Mutations in the interdomain linker region of DnaK abolish the chaperone action of the DnaK/DnaJ/GrpE system. FEBS Lett 497, 55–58.
Jiang JW, Prasad K, Lafer EM, Sousa R (2005). Structural basis of interdomain communication in the Hsc70 chaperone. Mol Cell 20, 513–524.
Jordan R, McMacken R (1995). Modulation of the ATPase activity of the molecular chaperone DnaK by peptides and the DnaJ and GrpE heat shock proteins. J Biol Chem 270, 4563–4569.
Kang PJ, Ostermann J, Shilling J, Neupert W, Craig EA, Pfanner N (1990). Requirement for Hsp70 in the mitochondrial matrix for translocation and folding of precursor proteins. Nature 348, 137–143.
Kaul SC, Deocaris CC, Wadhwa R (2007). Three faces of mortalin: a housekeeper, guardian and killer. Exp Gerontol 42, 263–274.
Kityk R, Kopp J, Sinning I, Mayer MP (2012). Structure and dynamics of the ATP-bound open conformation of Hsp70 chaperones. Mol Cell 48, 863–874.
Laloraya S, Gambill BD, Craig EA (1994). A role for a eukaryotic GrpE-related protein, Mge1p, in protein translocation. Proc Natl Acad Sci USA 91, 6481–6485.
Liberek K, Marszalek J, Ang D, Georgopoulos C, Zylicz M (1991a). *Escherichia coli* DnaJ and GrpE heat shock proteins jointly stimulate ATPase activity of DnaK. Proc Natl Acad Sci USA 88, 2874–2878.
Liberek K, Skowyra D, Zylicz M, Johnson C, Georgopoulos C (1991b). The *Escherichia coli* DnaK chaperone, the 70-kDa heat shock protein eukaryotic equivalent, changes conformation upon ATP hydrolysis, thus triggering its dissociation from a bound target protein. J Biol Chem 266, 14491–14496.
Liebscher M, Roujeinikova A (2009). Allosteric coupling between the lid and interdomain linker in DnaK revealed by inhibitor binding studies. J Bacteriol 191, 1456–1462.
Liu Q, D'Silva P, Walter W, Marszalek J, Craig EA (2003). Regulated cycling of mitochondrial Hsp70 at the protein import channel. Science 300, 139–141.
Liu Q, Krzewska J, Liberek K, Craig EA (2001). Mitochondrial Hsp70 Ssc1: role in protein folding. J Biol Chem 276, 6112–6118.
Mapa K, Sikor M, Kudryavtsev V, Waegemann K, Kalinin S, Seidel CA, Neupert W, Lamb DC, Mokranjac D (2010). The conformational dynamics of the mitochondrial Hsp70 chaperone. Mol Cell 38, 89–100.
Mayer MP, Bukau B (2005). Hsp70 chaperones: Cellular functions and molecular mechanism. Cell Mol Life Sci 62, 670–684.
McCarty JS, Buchberger A, Reinstein J, Bukau B (1995). The role of ATP in the functional cycle of the DnaK chaperone system. J Mol Biol 249, 126–137.
McCullum EO, Williams BA, Zhang J, Chaput JC (2010). Random mutagenesis by error-prone PCR. Methods Mol Biol 634, 103–109.
Montgomery DL, Morimoto RI, Gierasch LM (1999). Mutations in the substrate binding domain of the Escherichia coli 70 kDa molecular chaperone, DnaK, which alter substrate affinity or interdomain coupling. J Mol Biol 286, 915–932.
Moro F, Fernandez-Saiz V, Slutsky O, Azem A, Muga A (2005). Conformational properties of bacterial DnaK and yeast mitochondrial Hsp70—role of the divergent C-terminal alpha-helical subdomain. FEBS J 272, 3184–3196.
Neupert W, Brunner M (2002). The protein import motor of mitochondria. Nat Rev Mol Cell Bio 3, 555–565.
Neupert W, Hartl FU, Craig EA, Pfanner N (1990). How do polypeptides cross the mitochondrial-membranes? Cell 63, 447–450.
Neupert W, Herrmann JM (2007). Translocation of proteins into mitochondria. Annu Rev Biochem 76, 723–749.
Pareek G, Krishnamoorthy V, D'Silva P (2013). Molecular insights revealing interaction of tim23 and channel subunits of presequence translocase. Mol Cell Biol 33, 4641–4659.
Pareek G, Samaddar M, D'Silva P (2011). Primary sequence that determines the functional overlap between mitochondrial heat shock protein 70 Ssc1 and Ssc3 of *Saccharomyces cerevisiae*. J Biol Chem 286, 19001–19013.
Pfanner N, Geissler A (2001). Versatility of the mitochondrial protein import machinery. Nat Rev Mol Cell Biol 2, 339–349.
Qi RF *et al*. (2013). Allosteric opening of the polypeptide-binding site when an Hsp70 binds ATP. Nat Struct Mol Biol 20, 900–907.
Rehling P, Wiedemann N, Pfanner N, Truscott KN (2001). The mitochondrial import machinery for preproteins. Crit Rev Biochem Mol 36, 291–336.
Robzyk K, Kassir Y (1992). A simple and highly efficient procedure for rescuing autonomous plasmids from yeast. Nucleic Acids Res 20, 3790.
Rowley N, Pripbuus C, Westermann B, Brown C, Schwarz E, Barrell B, Neupert W (1994). Mdj1p, a novel chaperone of the Dnaj family, is involved in mitochondrial biogenesis and protein folding. Cell 77, 249–259.
Sickmann A *et al*. (2003). The proteome of *Saccharomyces cerevisiae* mitochondria. Proc Natl Acad Sci USA 100, 13207–13212.
Strub A, Zufall N, Voos W (2003). The putative helical lid of the Hsp70 peptide-binding domain is required for efficient preprotein translocation into mitochondria. J Mol Biol 334, 1087–1099.
Swain JF, Dinler G, Sivendran R, Montgomery DL, Stotz M, Gierasch LM (2007). Hsp70 chaperone ligands control domain association via an allosteric mechanism mediated by the interdomain linker. Mol Cell 26, 27–39.
Szabo A, Langer T, Schroder H, Flanagan J, Bukau B, Hartl FU (1994). The Atp hydrolysis-dependent reaction cycle of the *Escherichia coli* Hsp70 System Dnak, Dnaj, and Grpe. Proc Natl Acad Sci USA 91, 10345–10349.
Taylor RW, Turnbull DM (2005). Mitochondrial DNA mutations in human disease. Nat Rev Genet 6, 389–402.
Truscott KN *et al*. (2003). A J-protein is an essential subunit of the presequence translocase-associated protein import motor of mitochondria. J Cell Biol 163, 707–713.
Vogel M, Bukau B, Mayer MP (2006a). Allosteric regulation of Hsp70 chaperones by a proline switch. Mol Cell 21, 359–367.
Vogel M, Mayer MP, Bukau B (2006b). Allosteric regulation of Hsp70 chaperones involves a conserved interdomain linker. J Biol Chem 281, 38705–38711.
Voisine C, Craig EA, Zufall N, von Ahsen O, Pfanner N, Voos W (1999). The protein import motor of mitochondria: unfolding and trapping of preproteins are distinct and separable functions of matrix Hsp70. Cell 97, 565–574.
Voos W, vonAhsen O, Muller H, Guiard B, Rassow J, Pfanner N (1996). Differential requirement for the mitochondrial Hsp70-Tim44 complex in unfolding and translocation of preproteins. EMBO J 15, 2668–2677.
Zhuravleva A, Clerico EM, Gierasch LM (2012). An interdomain energetic tug-of-war creates the allosterically active state in Hsp70 molecular chaperones. Cell 151, 1296–1307.